

Enhanced Electrocatalytic Activity of Solvothermal Graphene Supported PtRu Catalyst toward Methanol Oxidation

Sungyool Bong¹, Byungchul Jang¹, Seunghee Woo² and Yuanzhe Piao^{1,3,*}

¹Graduate School of Convergence Science and Technology, Seoul National University, Suwon, 443-270, Republic of Korea

²Department of Chemistry, Seoul National University, Seoul, 151-747, Republic of Korea

³Advanced Institutes of Convergence Technology, Suwon, 443-270, Republic of Korea

*E-mail: parkat9@snu.ac.kr

Received: 9 April 2013 / Accepted: 12 May 2013 / Published: 1 June 2013

Solvothermal graphene (SG) in a bottom-up approach was used as a support, and a PtRu/SG catalyst was prepared by a modified impregnation method. The results showed that the PtRu nanoparticles were uniformly dispersed on the SG with average particle size of 2.6 nm. The PtRu/SG catalyst showed a large electrochemical active surface area ($59.95 \text{ m}^2 \text{ g}^{-1}$) and high catalytic activity toward oxidation of methanol.

Keywords: Solvothermal graphene, PtRu electrocatalyst, methanol, Electrooxidation

1. INTRODUCTION

Fuel cells have garnered wide interest as promising energy sources for the past several decades. In a fuel cell, the catalytic fuel oxidation is critical, because the energy provided by the fuel cell is limited by the ability of the catalyst [1]. Several types of carbon have been investigated in detail as catalytic supports in fuel cells, such as Vulcan XC-72R, carbon nanotubes (CNTs), graphene, and so on [2-4]. Due to their high electrical conductivity, high chemical stability, large surface area, and proper morphology [5-6], these materials are suitable supports for the catalysts in these respects.

Graphene is a good candidate as a support in fuel cells because its higher conductivity (10^3 – 10^4 S/m), good mechanical strength, and its large surface area (theoretical value, $2640 \text{ m}^2/\text{g}$) [7-10]. The modified Hummer's method is routinely used to obtain reduced graphene oxide (rGO) because of its low-cost, easy to carry out, and capable of mass production [11]. However, the functional sites on the rGO have low reduction efficiency when GO is reduced by using chemical and thermal methods.

Therefore, new method is required to preserve the theoretical properties of graphene. Solvothermal graphene (SG) could be an alternative to graphene produced using mechanical or Hummer's method due to its facile and low-priced gram-scale synthesis process. Moreover, it would also be possible to maintain the properties of the pristine graphene [12].

In this work, we investigated and verified the feasibility of a novel SG-supported electrocatalyst for methanol oxidation in an attempt to improve electrochemical behavior of the catalyst. The results showed that the SG-supported electrocatalyst showed improved catalytic activity toward methanol oxidation compared to that of a homemade Vulcan-supported catalyst.

2. EXPERIMENTAL

2.1 Preparation of SG

The SG was prepared and modified by the solvothermal method described by the Stride's group [12]. In a typical synthesis, sodium metal (2 g) and ethanol (5 ml) were placed into a Teflon-lined stainless-steel autoclave and they were synthesized solvothermally at 180 °C for 6 h. After cooling, the resulting materials were rapidly carbonized at 450 °C for 3 h, followed by washing with deionized water for 3 h and drying in an oven at 100 °C for 12 h. The mixture was carbonized again at 900 °C under a nitrogen atmosphere to produce the SG powder.

2.2 Preparations of PtRu/SG and PtRu/C composites

A 25 wt% PtRu/SG was synthesized with the modified impregnation method [13]. H_2PtCl_6 and RuCl_3 were used as metal precursors. The molar ratio of Pt and Ru was 1:1, and solvothermal graphene was used as a support to obtain PtRu/SG. A 25 wt% homemade PtRu/Vulcan XC-72R (=PtRu/C) was used as a reference catalyst in this experiment. The SG was mixed in aqueous solution containing appropriate amount of H_2PtCl_6 and RuCl_3 . Formaldehyde (molar ratio of HCHO: metal precursors = 20:1) was added to the suspension as a reducing agent. Basic solution, 1 M of sodium hydroxide was gradually dropped to the mixture until the pH value of 13. After the mixture was stirred for 15 min, HCl was inserted as a sedimentation promoter until pH 1 and stirred for 30 min. The solution was washed by distilled water and dried for overnight. The powder was heat-treated for 3 h at 300 °C under a mixed atmosphere of hydrogen and nitrogen.

2.3 Fabrication of PtRu/SG working electrode

Fabrication of PtRu/SG working electrode and electrochemical measurements: Electrochemical experiments were done with an electrochemical analyzer (Autolab PGSTAT302N), Ag/AgCl (Bioanalytical Systems, Inc.) as a reference electrode, a platinum wire as a counter electrode, and glassy carbon as a working electrode (3 mm in diameter, Bioanalytical Systems, Inc.). The electrocatalyst was suspended in appropriate amount of mixed solvent (5 wt% Nafion[®] solution, iso-

propyl alcohol and DI water), dropped onto the glassy carbon and dried under an IR lamp for 10 min. All the electrochemical measurements were performed in 0.5 M H₂SO₄ solution for blank and in a mixture of 1 M CH₃OH and 0.5 M H₂SO₄ for methanol oxidation. The electrochemically active surface area (ESA) of the PtRu/SG and PtRu/Vulcan XC-72R was determined using CO_{ad} stripping voltammetry in 0.5 M H₂SO₄ solution. CO adsorption was achieved at -0.97 V versus Ag/AgCl in a saturated CO solution for 10 min and the electrolyte was purged with nitrogen for another 10 min to remove CO on the surface.

2.4 Characterization

N₂ adsorption-desorption isotherms of SG were measured by a BELSORP-mini II (BEL JAPAN) nitrogen absorption analyzer. SG was analyzed with a micro-Raman system equipped with a homemade sample stage and a 514.5 wavelength laser line. The electrocatalyst was characterized by high resolution transmission electron spectroscopy (HR-TEM) measurements using a JEM-3000F (JEOL, Japan). Field-emission scanning electron microscopic (FESEM) images were obtained with a Hitachi S-4800 microscope and X-ray diffraction (XRD) analysis was made by using an X-ray diffractometer (M18XHFSRA, MAC science Co.).

3. RESULTS AND DISCUSSION

3.1 Characterization of the PtRu/SG composite

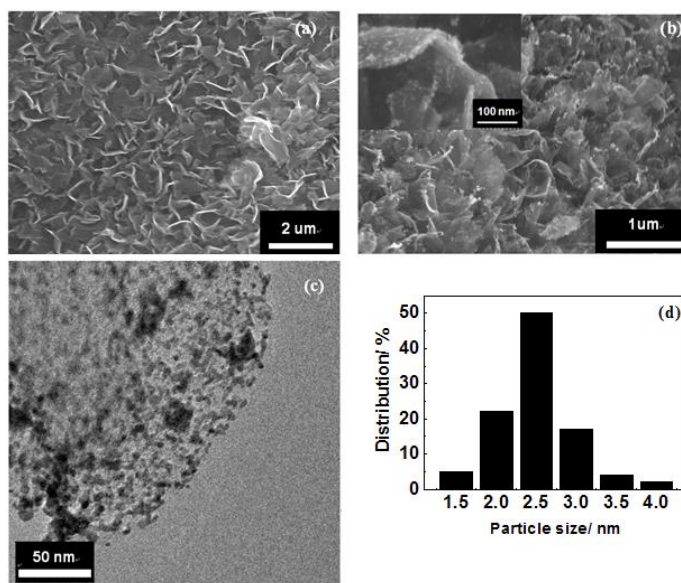


Figure 1. SEM image of SG (a), SEM images of PtRu/SG catalyst (inset is high resolution image) (b), HR-TEM image of PtRu/SG catalysts (c) and particle size distribution of PtRu/SG (d).

Fig. 1 shows FE-SEM and HR-TEM images of SG and PtRu/SG. As can be seen in Fig. 1(a), SG is composed of an assembly of thin graphene layers and hollow-shaped materials in the shape of a

broad blown. Fig. 1(b) and (c) show that the PtRu nanoparticles on the SG are well dispersed and have a small particle size. This means they have properties suitable for a support, such as a large effective BET surface area ($1509 \text{ m}^2/\text{g}$) and sufficient space to form metal nanoparticles, which result in good dispersion and small-sized metal nanoparticles as compared to Vulcan XC-72R with its $250 \text{ m}^2/\text{g}$ effective BET surface area. The PtRu nanoparticles had mean diameters of 2.6 nm and 3.3 nm on the SG and Vulcan XC-72R supports, respectively.

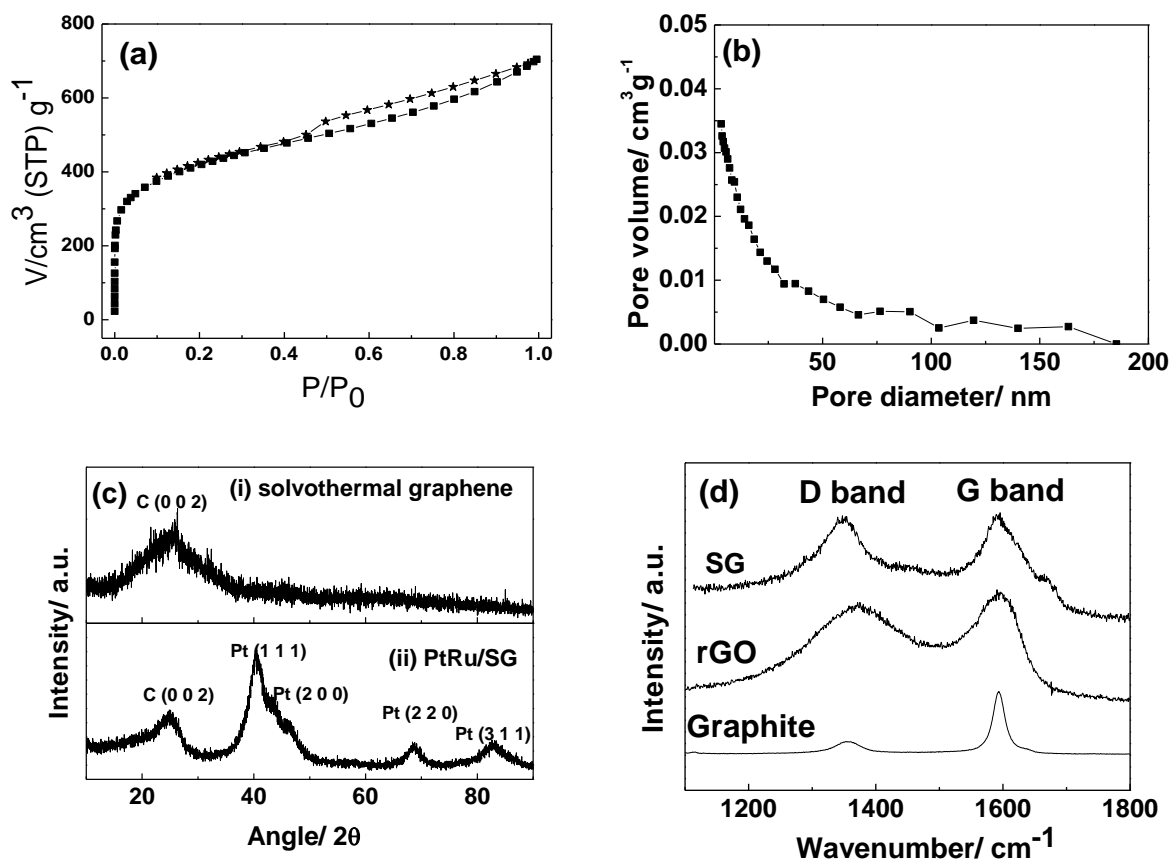


Figure 2. Nitrogen adsorption-desorption isotherms (a) and pore size distribution curves of the SG (b). XRD patterns of SG and PtRu/SG catalyst (c). Raman spectra of SG, rGO and graphite (d).

N_2 adsorption-desorption isotherms and the porosity of the SG are shown in Fig. 2(a) and (b). The Brunauer–Emmett–Teller (BET) specific surface area of the SG is $1592 \text{ m}^2/\text{g}$, indicating that the SG has a larger surface area than other carbon materials such as Hummers' graphene ($640 \text{ m}^2/\text{g}$) [14], CVD graphene ($174.4 \text{ m}^2/\text{g}$) [15], chemically modified graphene (CMG) ($706 \text{ m}^2/\text{g}$) [16], exfoliated graphene ($400 \text{ m}^2/\text{g}$) [17], and heat treated graphene ($600\text{--}900 \text{ m}^2/\text{g}$) [18], even though the specific surface area of the as-synthesized SG is smaller than the theoretical value for graphene ($2640 \text{ m}^2/\text{g}$).

SG exhibits a typical IV type isotherm hysteresis, which means that SG had a mesoporous system resulting from slit-shaped pores. Moreover, the total pore volume of the SG is as high as $1.11 \text{ m}^3/\text{g}$, which is much higher than that of Vulcan XC-72R ($0.35 \text{ m}^3/\text{g}$). These pores could provide enough mass-transport pathways for reactants and products.

Another goal was to estimate the nature of the SG and the SG-supported electrocatalyst. Fig. 2(c) shows the XRD patterns of the as-prepared catalysts. The XRD data confirm that the strong and slightly broad peak at $2\theta = 23.16^\circ$ for SG corresponds to rGO [19]. The Pt alloy (1 1 1) peak observed from these catalysts at a 2θ value of ca. 40° is shifted toward higher values compared to the bulk Pt reference peak, which indicates that an alloy is formed between platinum and ruthenium atoms [20]. The particle size of the PtRu/SG and PtRu/Vulcan catalysts was estimated using the Scherrer equation, and the lattice parameters were estimated from the XRD patterns according to Vegard's law:

$$\alpha = 2^{1/2} \lambda K_{\alpha 1} / \sin \theta_{\max},$$

where $\lambda K_{\alpha 1}$ is the X-ray wavelength of Cu $K_{\alpha 1}$ radiation (= 0.154056 nm) and θ_{\max} is the peak position. The degree of alloying in the PtRu/SG and Vulcan electrocatalysts was calculated from the fraction of Ru atoms in the alloy, χ_{Ru} [21,22]

$$a = a_0 - 0.124 \chi_{\text{Ru}}$$

where χ_{Ru} is the lattice parameter of the catalyst and $a_0 = 0.39155$ nm is the lattice parameter. The XRD patterns of the catalysts on the SG and Vulcan supports were measured to confirm the degree of PtRu alloying and to calculate the average particle size. All catalysts exhibited peaks at around $2\theta = 40^\circ$, 47° , 67° , and 83° that correspond to the (1 1 1), (2 0 0), (2 2 0), and (3 1 1) diffractions of the face-centered cubic (fcc) structure of Pt, respectively. The particle sizes of these catalysts were calculated according to the Scherrer equation, and the lattice parameter was determined by Vegard's law [23].

Table 1. The Pt (1 1 1) peak position, lattice parameter, calculated particle size and average particle size.

Catalysts	(1 1 1) Peak position/ 2θ	Lattice parameter/ Å	XRD particle size/ nm	TEM particle size/ nm
PtRu/SG	40.47	3.867	2.6	2.5±0.25
PtRu/VC	40.36	3.872	3.3	3.4±0.41

Table 1 (a) summarizes the Pt (1 1 1) peak positions, lattice parameters, calculated particle sizes, and average particle sizes from the XRD and HR-TEM data. The as-prepared catalyst showed a good alloy state based on the blue- shift of the lattice parameter relative to the Pt value (lattice parameter = 0.39155 nm), and the particle size calculated from the XRD data was in good agreement with the average particle size from the HR-TEM image. The XRD and TEM data also confirm that the PtRu/SG catalysts had metal particles uniformly dispersed onto the SG support. Fig. 2(d) shows the Raman spectra of the SG along with information about the distinction between graphite and graphene, the difference between GO and rGO in terms of the ratio between the D and G bands, and the number of layers. The Raman spectrum shows that the ratio between the D (1352 cm^{-1}) and G (1593 cm^{-1}) bands is similar to those of highly defective graphite and reduced graphene oxide (rGO) [24].

3.2 Electrochemical behavior of the PtRu/SG electrode

It is well known that the electrochemical behavior can be explained by certain unique parameters of the material. Fig. 3(a) shows the cyclic voltammograms of these catalysts in 0.5 M H₂SO₄ solution. The electric double layer capacitance (EDLC) is dependent on the specific area of the support. The PtRu/SG catalyst has thick double-layer areas because of the intrinsic properties of graphene [25]. The electrochemical active surface area (EAS) of the Pt-based catalysts is usually determined by measuring the electrochemical hydrogen adsorption and desorption. However, this method cannot be used for PtRu/C catalysts because of the thick electric double layer.

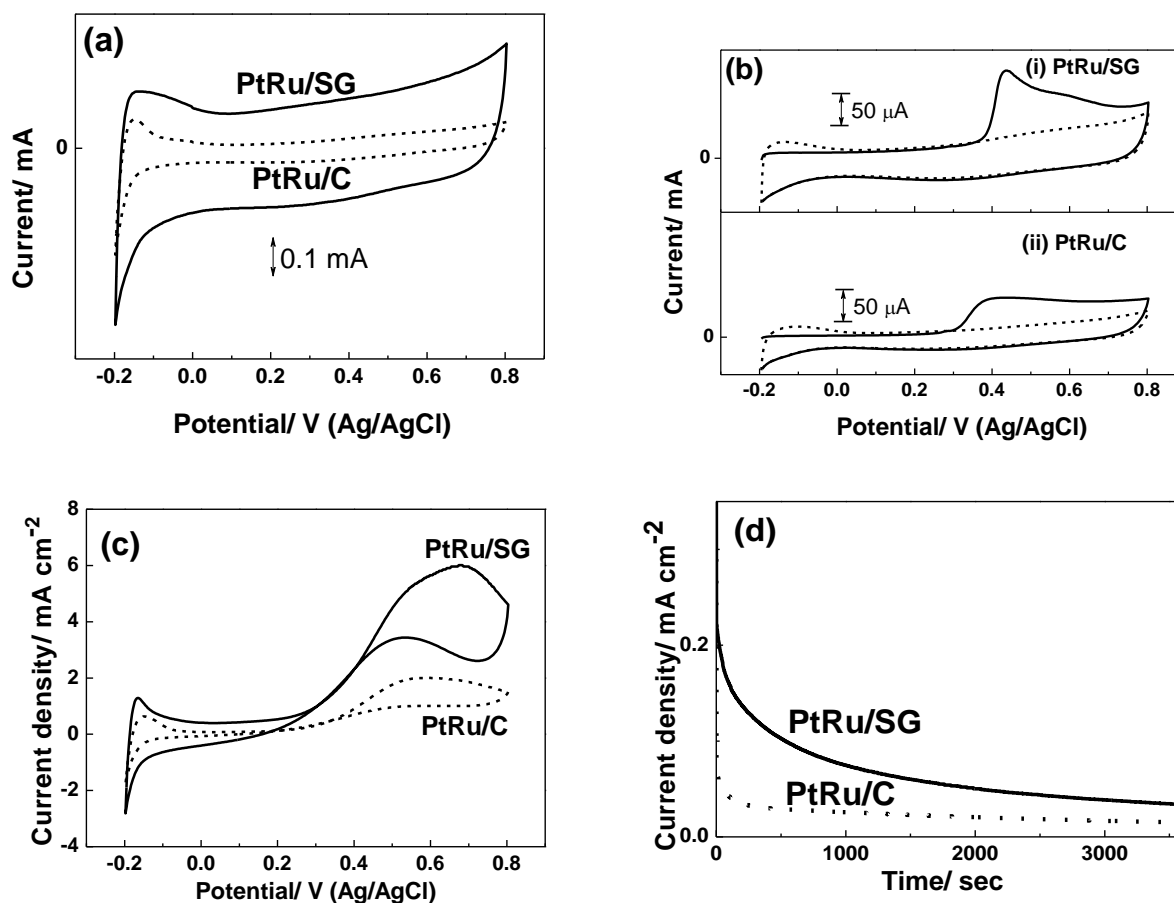


Figure 3. (a) Cyclic voltammogram of PtRu/SG and PtRu/C in 0.5 M H₂SO₄ at a scan rate of 50 mV/sec, (b) CO_{ads} stripping cyclic voltammograms and (c) cyclic voltammograms in 1 M CH₃OH and 0.5 M H₂SO₄. (d) Chronoamperometric curves in 1 M CH₃OH and 0.5 M H₂SO₄ at 0.6 V for 3600 sec.

Instead, CO-stripping voltammetry can be very useful for measuring the EAS. The EAS is dependent on not only the metal particle size and distribution, but also the bifunctional catalytic mechanism [26]. Fig. 3(b) shows the CO-stripping voltammograms of the prepared catalysts. According to these electrochemical results, the EAS of the PtRu/SG (59.95 m² g⁻¹) is much larger than that of the PtRu/C (25.28 m² g⁻¹). As mentioned above, the PtRu/SG catalyst has small-sized metal

nanoparticles with a very narrow size distribution as compared to the PtRu/C, which might affect the EAS in the CO-stripping measurements [27].

The electrochemical behavior of the prepared catalysts toward methanol oxidation was evaluated, as shown in Fig. 3(c). The PtRu/SG catalyst exhibited an activity about 3-fold higher than that of the PtRu/C. Finally, the stability of these catalysts during methanol oxidation was demonstrated, and the current was found to be slightly higher for the SG-supported catalyst than for the VC-supported catalyst. Furthermore, the current decreased less for the PtRu/SG than for the PtRu/C after 3600 s, as shown in Fig. 3(d). According to Guo's report, the existence of a long-term poisoning rate (δ) implies that the durability is determined by a linear decay of the current for a period of more than 500 s, as shown by the following equation:

$$\delta = \frac{100}{I_0} \times \left(\frac{dI}{dt} \right)_{t > 500 s} (\% s^{-1}),$$

where $(dI/dt)_{t > 500 s}$ is the slope of the linear portion of the decay current and I_0 is the starting current of the polarization extrapolated from the linear current decay. The δ values for PtRu/SG and PtRu/C are 0.015 and 0.022, respectively. The SG-supported catalyst has a lower poisoning rate, which in turn explains its high tolerance to CO and other intermediate species generated during the oxidation of methanol. Thus, the SG-supported catalyst can achieve long-term stability [28].

According to a previous report by Dicks, the requirements for carbon as a supporting material in fuel cells are large surface area, high electrical conductivity, proper chemical stability, and low cost [5]. The SG has a high surface area (1509 m²/g) compared to commercial rGO (833 m²/g, Graphene supermarket, USA). Kaner group reported that graphene has a sp² structure, which means fast electron transport in the graphene and rigid framework [29]. Stride et al. reported that gram-scale production of SG might be achieved with comparative ease [8]. These results imply that SG is a good candidate as supporting material for electrocatalysts in fuel cells.

4. CONCLUSIONS

The role of carbon as a support in electrocatalytic reactions is very crucial, since its properties strongly affect the electrocatalytic activity. We introduced SG as a support to improve the electrochemical activity of the supported catalyst. The PtRu/SG catalyst has enhanced properties due to its sufficient surface area and suitable structure. It was observed that the PtRu/SG has a large EAS as well as remarkable electrocatalytic activity and durability during methanol oxidation.

ACKNOWLEDGEMENTS

This work was supported by the Center for Integrated Smart Sensors funded by the Ministry of Education, Science and Technology as Global Frontier Project (CISS-2012M3A6A6054186) and by the Basic Science Research Program through the National Research Foundation of Korea (NRF) funded by the Ministry of Education, Science and Technology (No. 2012-0008330).

References

1. Z. Yan, M. Wang, B. Huang, R. Liu, J. Zhao, *Int. J. Electrochem. Sci.*, 8 (2013) 149.

2. H. Huang, H. Chen, D. Sun and X. Wang, *J. Power Sources*, 204 (2012) 46.
3. N. Kakati, J. Maiti, S. H. Jee, S. H. Lee and Y. S. Yoon, *J. Alloys Compd.*, 509 (2011) 5617.
4. R. N. Bonifácio, A. O. Neto, M. Linardi, *Int. J. Electrochem. Sci.*, 8 (2013) 159.
5. A. L. Dicks, *J. Power Sources*, 156 (2006) 128.
6. S. Bong, S. Uhm, Y.-R. Kim, J. Lee and H. Kim, *Electrocatal.*, 1 (2010) 139.
7. D. R. Dreyer, S. Park, C. W. Bielawski and R. S. Ruoff, *Chem. Soc. Rev.*, 39 (2010) 228.
8. R. Kou, Y. Y. Shao, D. H. Wang, M. H. Engelhard, J. H. Kwak, J. Wang, V. V. Viswanathan, C. M. Wang, Y.H. Lin, Y. Wang, I.A. Aksay and J. Liu, *Electrochem. Commun.*, 11 (2009) 954.
9. J. D. Roy-Mayhew, D. J. Bozym, C. Punckt and I. A. Aksay, *ACS Nano*, 4 (2010) 6203.
10. S. J. Guo, S. J. Dong and E. W. Wang, *ACS Nano*, 4 (2010) 547.
11. N. I. Kovtyukhova, P. J. Olliver, B. R. Martin, T. E. Mallouk, S. A. Chizhik, E. V. Buzaneva and A. D. Gorchinskiy, *Chem. Mater.*, 11 (1999) 771.
12. M. Choucair, P. Thordarson and J. A. Stride, *Nat. Nanotech.*, 4 (2009) 30.
13. I. Kim, S. Bong, S. Woo, R. K. Mahajan and H. Kim, *Int. J. Hydrogen Energ.*, 36 (2011) 1803.
14. G. Srinivas, Y. Zhu, R. Piner, N. Skipper, M. Ellerby and R. Ruoff, *Carbon*, 48 (2010) 630.
15. E. Dervishi, Z. Li, F. Watanabe, A. Biswas, Y. Xu, A. R. Biris, V. Saini and A. S. Biris, *Chem. Commun.*, (2009) 4061.
16. M. D. Stoller, S. Park, Y. Zhu, J. An and R. S. Ruoff, *Nano Lett.*, 8 (2008) 3498.
17. W. Lv, D.-M. Tang, Y.-B. He, C.-H. You, Z.-Q. Shi, X.-C. Chen, C.-M. Chen, P.-X. Hou, C. Liu and Q.-H. Yang, *ACS Nano*, 3 (2009) 3730.
18. M. J. McAllister, J.-L. Li, D. H. Adamson, H. C. Schniepp, A. A. Abdala, J. Liu, M. Herrera-Alonso, D. L. Milius, R. Car, R. K. Prud'homme and I. A. Aksay, *Chem. Mater.*, 19 (2007) 4396.
19. S. Bong, Y.-R. Kim, I. Kim, S. Woo, S. Uhm, J. Lee and H. Kim, *Electrochem. Commun.*, 12 (2010) 129.
20. J. Guo, G. Sun, Q. Wang, G. Wang, Z. Zhou, S. Tang, L. Jiang, B. Zhou and Q. Xin, *Carbon*, 44 (2006) 152.
21. E. Antolini and F. Gardellini, *J. Alloys Compd.*, 315 (2000) 118.
22. E. Antolini, L. Giorgi, F. Cardellini and E. Passalacqua, *J. Solid State Electrochem.*, 5 (2001) 131.
23. V. Radmilovic, H. A. Gasteiger, P. N. Ross, *J. Catal.* 154 (1995) 98.
24. H. Shin, K. K. Kim, A. Benayad, S. Yoon, H. K. Park, I. Jung, M. H. Jin, H. Jeong, J. M. Kim, J. Choi and Y. H. Lee, *Adv. Funct. Mat.*, 19 (2009) 1987.
25. H. P. Dhar, L. G. Christner, A. K. Kush, *J. Electrochem. Soc.*, 134 (1987) 3021.
26. M. Watanabe and S. Motoo, *J. Electroanal. Chem.*, 60 (1975) 259.
27. H. Uchida, K. Izumi and M. Watanabe, *J. Phys. Chem. C*, 110 (2006) 21924.
28. J. W. Guo, T. S. Zhao, J. Prabhuram, R. Chen and C. W. Wong, *Electrochim. Acta*, 51 (2005) 754.
29. M. J. Allen, V. C. Tung and R. B. Kaner, *Chem. Rev.*, 110 (2010) 132.